

The Density of Cholinergic Receptors at the Endplate Postsynaptic Membrane: Ultrastructural Studies in Two Mammalian Species

C. W. Porter* and E. A. Barnard**

Departments of Biochemistry and Pathology, State University of New York,
Buffalo, New York 14214

Received 5 July 1974

Summary. Electron-microscope autoradiography of diaphragm endplates of the American brown bat, labeled to saturation with tritiated α -bungarotoxin, has been used as a means to localize and quantitate the acetylcholine receptor there. Analysis of the grain distribution in these autoradiographs reveals that the receptor sites in this endplate are located on the postsynaptic membrane at an average density of $8,800/\mu^2$. The sites are distributed asymmetrically along that membrane, being concentrated at the crests of the postjunctional folds—that portion nearest to the presynaptic membrane. The receptor site density at these regions of the postsynaptic membrane is estimated to be $20,000$ – $25,000/\mu^2$ of membrane surface. A comparison of these membrane site densities with those of endplates of red and white fibers of the mouse reveals a close similarity. On this basis, it is suggested that the receptor site density at the crests of the folds may be a characteristic feature of endplates of vertebrates.

In contrast to the acetylcholine receptor sites, cholinesterase sites (determined autoradiographically in ^3H -diisopropylfluorophosphate-labeled endplates) are largely distributed in a uniform manner over the postjunctional folds. The function of the secondary folds is, therefore, reassessed. Ultrastructural evidence available from other laboratories on the spatial characteristics of transmitter release and of postsynaptic dense particles is in accord with a model drawn for this molecular architecture at the vertebrate endplate.

In a previous study (Porter, Barnard & Chiu, 1973a), it was shown that the snake venom toxin, α -bungarotoxin (α -BuTX), in tritiated form, can be applied to the ultrastructural localization of the acetylcholine (ACh) receptor sites at motor endplates. In that study, which employed mouse diaphragm muscle labeled thus, electron-microscope (EM) autoradiographs were prepared, and the labeling therein was shown to be consistent with a postsynaptic location of the α -BuTX-binding sites. That toxin is known from a variety of pharmacological and biochemical studies (for a review *see* Lee,

* *Present address:* Dept. of Experimental Therapeutics, Roswell Park Memorial Institute, Buffalo, New York 14203.

** Correspondence and reprint requests should be addressed to this author at the Dept. of Biochemistry, SUNY.

1972) to be a highly specific and essentially irreversible reagent for the nicotinic ACh receptor. The ^3H -diacetyl derivative of $\alpha\text{-BuTX}$ ($^3\text{H}\text{-}\alpha\text{-BuTX}$), used in this work, has been shown to be unchanged from native $\alpha\text{-BuTX}$ in specificity and reactivity for the endplate ACh receptor (Barnard, Wieckowski & Chiu, 1971; Albuquerque, Barnard, Chiu, Lapa, Dolly, Jansson, Daly & Witkop, 1973; Chiu, Lapa, Barnard & Albuquerque, 1974).

The *average* membrane density of the $\alpha\text{-BuTX}$ -binding sites, assumed to be the active centers of the ACh receptors, was determined in the ultrastructural study of mouse diaphragm and found to be 8,400 per μ^2 of postsynaptic membrane (Porter *et al.*, 1973*a*). It is now known (Albuquerque, Barnard, Porter & Warnick, 1974; Fertuck & Salpeter, 1974) that these sites are more concentrated at and near the crests¹ or tops of the junctional folds; we present here an analysis of the local densities of the receptor sites along these membranes. The significance of such density determinations is of importance in understanding the primary molecular events of synaptic transmission. For example, it has been determined (Albuquerque *et al.*, 1974) that the sensitivity of the endplate to applied ACh is determined by the receptor density and not by the total number of receptors at the endplate.

Further, we have thought it important to compare these densities at the endplates of another mammalian species phylogenetically distant from the mouse. This will provide one piece of evidence on the generality of this molecular arrangement in the motor endplate. For this purpose, we have found it convenient to employ the American brown bat. The evidence obtained here adds support to the view that the average fold crest density of 22,000 receptor sites/ μ^2 is generally characteristic of the mammalian endplate postsynaptic membrane there. One portion of this work has been reported elsewhere (Albuquerque *et al.*, 1974; Porter & Barnard, 1974) in a much less detailed form.

Materials and Methods

^3H -Diacetyl- $\alpha\text{-BuTX}$ (4.1 C/mmmole) was prepared by the method used previously (Barnard *et al.*, 1971; Porter, Chiu, Wieckowski & Barnard, 1973*b*). An American big brown bat (*Eptesicus fuscus*), weighing 14 g, was collected locally; it was given a supralethal dose (1.5 $\mu\text{g/g}$ body wt) of $^3\text{H}\text{-BuTX}$ via the saphenous vein of the wing. Upon death (10 min post-injection) the diaphragm was thoroughly washed, fixed in 3% glutaraldehyde (2 hr at 4 °C, pH 7.4) and small innervated areas were removed for

¹ We use the term "crest" to refer to that region of a folded postsynaptic membrane which unites the upper (juxta-neuronal) walls of two adjacent folds, and which normally has some convexity towards the apposed presynaptic membrane. It is shown illustratively in Fig. 6. For a discussion of the range of fold morphology in endplates of different vertebrate muscles, to which the concept of the crest must be adapted, see Fardeau (1973) and Zacks (1973).

embedding in Epon-Araldite. That this mode of tissue labeling achieves saturation binding of α -BuTX has been established (in mice) in analysis by liquid scintillation counting and by light microscope autoradiography of the endplates (Barnard *et al.*, 1971; Chiu *et al.*, 1974).

The EM autoradiographic methods used followed precisely those described previously (Porter *et al.*, 1973*a*). Over 100 autoradiographs of endplates were used in the analysis of the bat endplates. For the mouse diaphragm, the blocks of labeled muscle prepared previously (Porter *et al.*, 1973*a*) were used, but more sections were cut and a larger number of endplate profiles (~ 200) than hitherto was analyzed.

Grain densities at varying distances from the axonal or postjunctional membrane were obtained as previously described (Porter *et al.*, 1973*a*). A uniform grid of points (1 point $\equiv 0.5 \mu^2$ at $30,000\times$) was again used in determining the areas involved. The grain densities were tabulated for columns each 1600 \AA wide on either side of the given membrane—those on the axon side being given a negative sign, and those on the muscle side a positive sign. The distances from the membrane were expressed in units of half-distance (HD).² Finally, the density in the column containing the line source (HD = 0) was set equal to unity, and all other columns were adjusted proportionally. When, instead, the distribution of label along the folds was analyzed, only those grain densities immediately over the areas where the postjunctional membrane is infolded (postjunctional folds) were used; all the grains there lying in a band enclosing folded regions of this membrane were counted, up to the axonal membrane as the limit. The corresponding areas were measured by the lattice method, and these densities were normalized in the usual manner.

Absolute quantitation of the binding sites on the postjunctional membrane was made on the basis that one α -BuTX molecule binds irreversibly to one ACh receptor active center. In determining the number of receptor sites, firstly all of the grains attributable to sites on the postjunctional membrane (i.e. the number of grains lying under the theoretical distribution curve in Fig. 3*A* for a source on that membrane, minus the corresponding background count) were taken in relation to the total length of that membrane present in the same autoradiographs. The membrane surface areas were determined by tracing all these recognizable membrane profiles with a map measurer, and multiplying their total length by the known section thickness. For the batch of Ilford L-4 emulsion and the development used, and the magnitude of the radiation dose over the zone in question here ($0.4 \text{ grains}/\mu^2$ over the cleft substance), the sensitivity was shown to be 1 grain per 10.0 radioactive decays. [This latter calibration was performed by Dr. G. C. Budd (Toledo, Ohio) on samples of this emulsion batch exposed to a tritiated standard, at this same radiation dose.] From this sensitivity value, the specific radioactivity of the ^3H - α -BuTX employed, and the emulsion exposure period, the number of molecules involved is at once obtained; this, with the corresponding area of the postjunctional membrane, yielded the average density of α -BuTX-binding sites per μ^2 of membrane (Porter *et al.*, 1973*a*).

Results

α -BuTX-Binding Sites at Endplates of the Bat Diaphragm

The following results are based on an analysis of endplates from the diaphragm of a single animal. Four tissue blocks, containing a minimum of

² HD is an experimental measure of resolution for a given autoradiographic system; it indicates the distance from a radioactive line source within which 50% of the developed grains fall. In this study, 1 HD = 1600 \AA . For further details, see Salpeter *et al.* (1969).

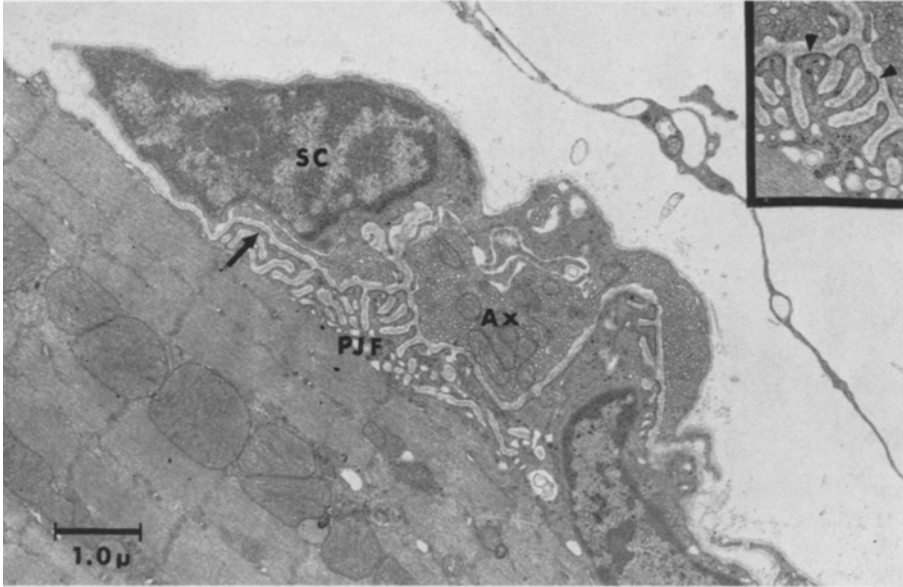


Fig. 1. Electron-micrograph of a portion of a bat diaphragm endplate, treated *in vivo* with $^3\text{H-}\alpha\text{-BuTX}$ but not processed for autoradiography. The postjunctional folds (PJF) are shorter than those seen at mouse diaphragm endplates and display a greater tendency to interconnect to form loops (arrow). The axon (Ax) is attached to the side of the fiber and not embedded in it. No structural changes attributable to the toxin were noted. The inset is an enlarged portion of the postjunctional fold zone, showing the thickened region of the postsynaptic membrane (arrowheads) at the fold crests. (SC, Schwann cell). 15,000 \times

three endplates per initial section, were utilized for the EM autoradiography. Numerous sections were taken from 3 or 4 regions at least 100 μ apart, so as to ensure new endplate samples at every new level of sectioning.

The muscle fibers of the bat diaphragm are, like those of the mouse, predominantly red in type (Gauthier & Padykula, 1966), and by our measurements made by light microscopy of the muscle used, they are approximately 21 μ in diameter. Certain subtle differences from the mouse diaphragm endplate were noted. The sarcoplasmic trough, which normally receives the terminal axon, is either absent or very shallow at the bat endplate. The axon, therefore, gives the appearance of being attached to the side of the muscle fiber rather than embedded in it. In addition, the folds of the subneural apparatus (average depth 0.35 μ) are not as deep as those in the mouse diaphragm (0.50 μ), and they display a noticeable tendency to interconnect to form loops (Fig. 1). These differences were reflected in the ratio of postsynaptic to axonal presynaptic membrane lengths per endplate, which

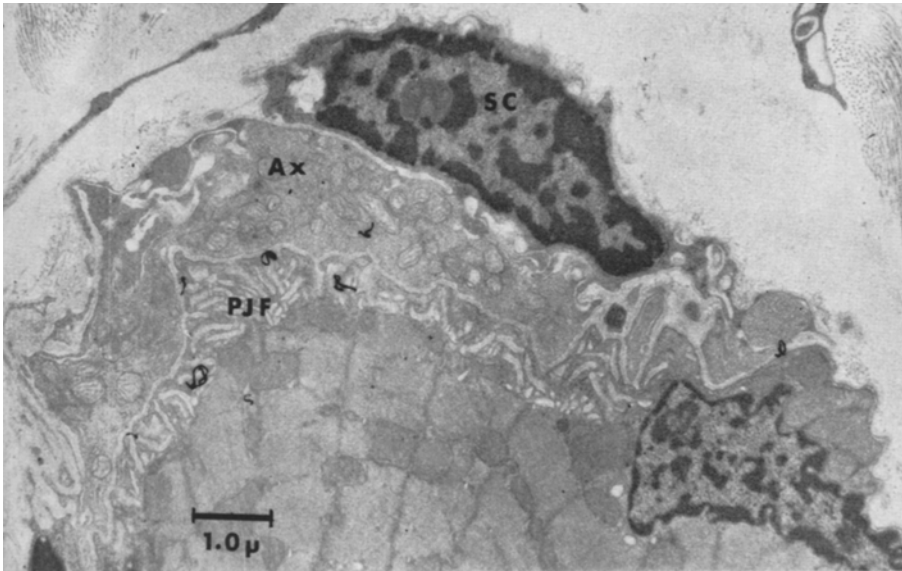


Fig. 2. Electron-microscope autoradiograph of a portion of a bat diaphragm endplate labeled with $^3\text{H-}\alpha\text{-BuTX}$. The silver grains lie over the postjunctional folds (PJF) or within the range of radiation scatter from them (Ax, axon; SC, Schwann cell). $14,000\times$

were measured here (Table 1, column 2). As in the mouse, no morphological changes were observed as a result of the intoxication.

A typical autoradiograph of a $^3\text{H-}\alpha\text{-BuTX}$ -labeled bat endplate is shown in Fig. 2. The general pattern of the labeling in this muscle with the grains concentrated over the subneural apparatus of the endplate or in the adjacent zone of radiation scatter from it, was as noted for the mouse diaphragm (Porter *et al.*, 1973*a*). Also as in the mouse, the grain density distributions, when plotted as a function of distance from either the postsynaptic (Fig. 3*A*) or the axonal presynaptic membrane (Fig. 3*B*), were as expected for radiation emanating from the postjunctional membrane. The grain spread seen

Table 1. Average $\alpha\text{-BuTX}$ binding site densities at bat and mouse diaphragm endplates

Membrane	Folding ratio ^a	Binding sites
Postjunctional (bat)	4.5	$8,800/\mu^2$
Postjunctional (mouse)	3.0	$8,400/\mu^2$
Sarcolemma		$180/\mu^2$

^a The ratio of the total lengths of postsynaptic to presynaptic membrane as measured in our electron-micrographs of these endplates.

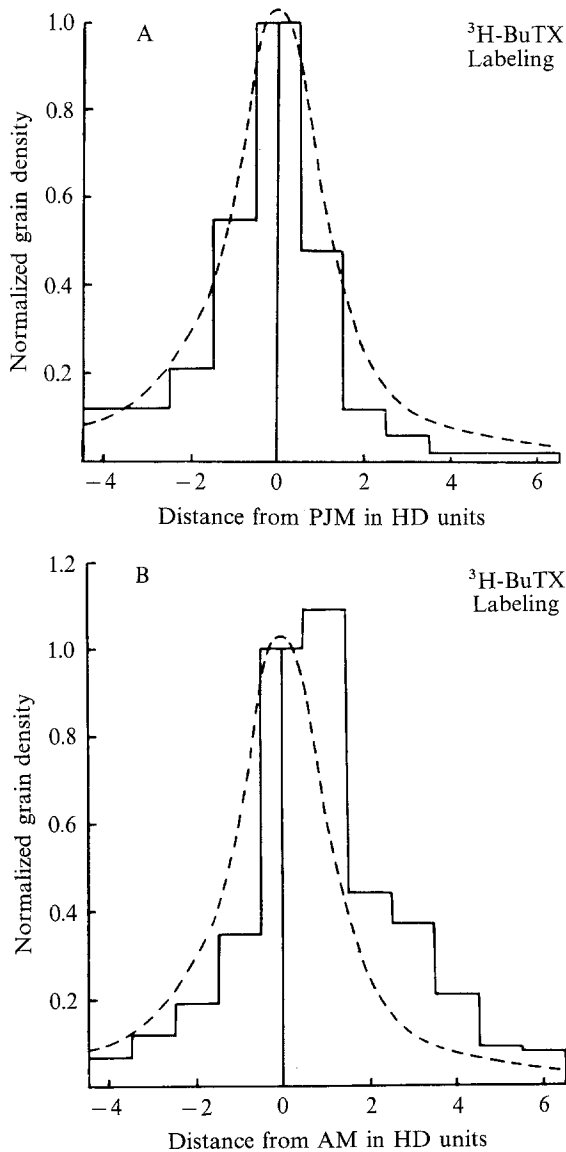


Fig. 3. (A) Histogram showing the distribution of silver grains around the *postjunctional* membrane (PJM) for bat diaphragm endplates labeled with $^3\text{H-}\alpha\text{-BuTX}$ (based on 334 grains and 2,400 points). Note that the experimental distribution agrees closely with the expected distribution curve (broken line) for a source located on the postjunctional membrane. (The theoretical curve was derived according to Salpeter *et al.* (1969), and is adjusted on the axonal side for the average, slight asymmetry of the bat endplate trough.) HD (half-distance) units are a measurement of autoradiographic resolution (*see* footnote 2). Negative values of HD designate distances on the axon side of the postjunctional membrane (HD=0), and positive values on the muscle side. (B) Histogram of grain densities around the *axonal* membrane (AM) for bat diaphragm endplates labeled with $^3\text{H-}\alpha\text{-BuTX}$ (based on 325 grains and 2,000 points). The grain scatter does not at all fit the theoretical curve for the grain distribution from a source centered on the axonal membrane (HD=0). Instead, the grain densities are distributed over the region on the muscle side of the axonal membrane (positive HD units) largely corresponding to the crests of the postjunctional folds

around the postsynaptic membrane agrees closely with a curve drawn for the theoretical grain distribution for a radioactive line source (Salpeter, Bachmann & Salpeter, 1969) coincident with that membrane. When plotted, on the other hand, with the axonal membrane as origin, the grain density is distributed over an area on the muscle side of the presynaptic membrane corresponding to the junctional folds. The narrow width of this zone is attributed to the shallow folds characteristic of the bat endplate and to a concentration of the receptors at the crests of the folds.

The contrast between the two distributions plotted in Fig. 3, in which the grain density follows the postsynaptic membrane quite faithfully despite its complex contours, indicates (as before) that the radioactivity is bound to this postsynaptic membrane and, at least for the bulk of it, not with the axonal membrane. This conclusion is substantiated by the results of other studies on mouse muscle (Porter & Barnard, 1974), which show that removal of the cleft substance and/or the terminal axon by either proteolytic enzyme digestion or by denervation fails to change the grain density or distribution over the folds in such autoradiographs. However, in neither set of results would one distinguish a low but significant level of labeling at the presynaptic membrane, say of the order of 10% or less of that at the postsynaptic membrane; hence, a receptor population there of that order is not excluded.

Fig. 4 is a plot made to include only those grain densities exclusively over the folds. This gives a more accurate representation of the true grain density distribution over the folds than does Fig. 3B, where all density determinations on the muscle side of the axonal membrane are employed, including those for grains not over the postjunctional folds (e.g. grains in areas apposing the axonal membrane where the postjunctional membrane does not contain secondary folds). This inclusion dilutes (due to normalization) the true grain density over the postsynaptic areas more distant from the axonal membrane, such as those encountered in oblique sections of the endplate, and thereby gives a false impression of low grain densities at some of those areas (Fig. 3B). Fig. 4 clearly demonstrates that the labeling is asymmetrically distributed over the folds. A similar analysis was made in the case of the ^3H - α -BuTX-labeled mouse diaphragm (Fig. 5), with the same result.³ In the cases of both muscles, the region of highest grain

³ In the previous study of the mouse diaphragm (Porter *et al.*, 1973a), the same effect was apparent but seen less clearly than here. Significance was not attached to it in that report, due to the relatively small number of grains involved. A larger number of grains and points were accumulated over the fold region of the mouse diaphragm endplate sections in the course of the present study, permitting the asymmetry to be unambiguously recognized. We have recently noted this latter finding in another report (Albuquerque *et al.*, 1974).

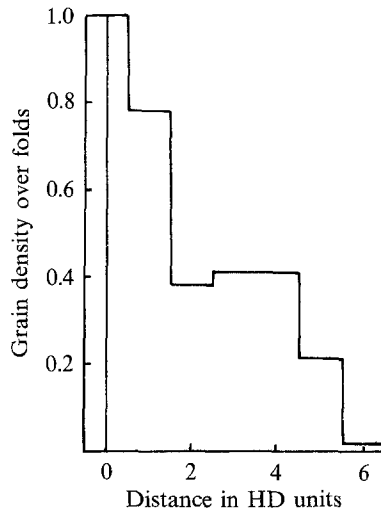


Fig. 4. Experimental grain densities *over the postjunctional folds* plotted in relation to distance down the folds from the *axonal* membrane (HD = 0) for bat diaphragm end-plates (based on 260 grains and 1,200 points). Only those grains and points lying over a profile of postsynaptic membrane or the associated cleft, whether that membrane was folded or not, were included in this analysis; *see* Materials and Methods for further details. (The first bin, HD = $-1/2$ to HD = $+1/2$, is not strictly comparable to the other bins, in this form of the analysis. It contains most of the grain contribution from any unfolded segments of the postjunctional membrane present, but is reduced in density by the inclusion of a half-bin corresponding to the axonal side, and by a small width (~ 500 Å) due to the primary synaptic cleft. These two distorting effects in opposite directions appear approximately to cancel each other.) The grain densities at the fold depths (HD 4 to 6) are greater than expected for radiation scatter from isotope on the fold crests (HD 0 to 2)

density corresponds to the crests of the junctional folds, i.e. that area of postsynaptic membrane apposing or next nearest to the presynaptic membrane. By comparison, the zone of the histogram representing the depths of the folds (i.e. over the range HD = 4 to 6, for the great majority of the grains there) has considerably fewer receptor sites. When the effect of radiation scatter from the crests of the folds is considered (on the same basis as in Fig. 3), it is estimated that the fold depths contain less than one-sixth of the binding site density found at their tips.

The decrease in labeling of the bat postsynaptic membrane that is seen as it becomes more distant from the presynaptic membrane (Fig. 4) is much more rapid than in the case of the mouse muscle (Fig. 5). However, since the junctional folds of the bat muscle are considerably shallower than those of the mouse (*see above*), and since there is a corresponding reduction there in the extent of the postsynaptic membrane that has the electron-dense

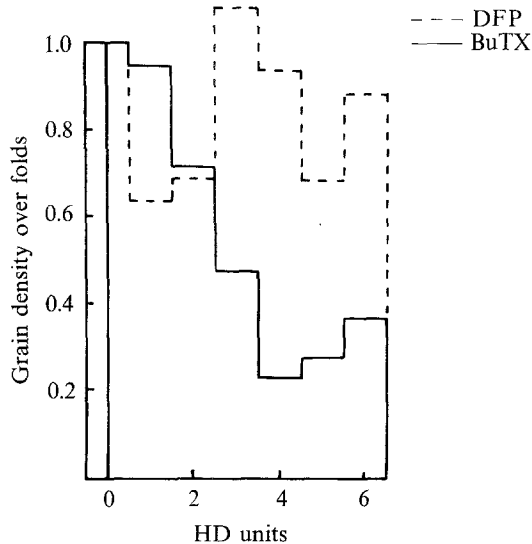


Fig. 5. Grain density distributions over the region of postjunctional folds for mouse diaphragm endplates labeled with $^3\text{H-}\alpha\text{-BuTX}$ or with $^3\text{H-DFP}$. In contrast to the ACh receptor sites which are concentrated at the crests of the folds, the cholinesterases (DFP-sensitive sites) are distributed evenly over the folds. Data used in formulating this histogram are taken from previous studies (Porter *et al.*, 1973*b*; Albuquerque *et al.*, 1974). (BuTX plot is based on 510 grains and 1,400 points; DFP plot is based on 200 grains and 550 points)

“thickening” (see Fig. 1, inset), which has been suggested (Birks, Huxley & Katz, 1960) to correspond to the receptor molecules, this finding is as expected.

Density of the Binding Sites on the Membranes

As noted above, the histogram data are taken to indicate that, as in the mouse, the receptors are located (within the limits of this technique) on the postsynaptic membrane. All of the grains related to that membrane, therefore, were employed, together with the corresponding total length of postsynaptic membrane, to obtain the average density. This value was $8,800/\mu^2$ of postsynaptic membrane. This density is indistinguishable from that found previously for the mouse (Table 1). The density of $\alpha\text{-BuTX}$ binding sites along the nearby sarcolemma is seen to be negligible in comparison with that at the postjunctional membrane, even though the two are continuous. Clearly, then, the concentration of receptor sites at the motor endplate is not brought about simply by the increased folding of the membrane in that region.

Comparison with Cholinesterase Distribution

The complement of total cholinesterase-like (ChE-like) active centers at the endplate can be determined by reaction with labeled diisopropylfluorophosphate (DFP) under specified conditions, followed by autoradiography (Barnard & Rogers, 1967; Salpeter, 1969). The acetylcholinesterase (AChE) sites that contribute to this total can then be localized separately by the use of specific reactivation by pyridine-2-aldoxime methiodide (2-PAM). In the mouse sternomastoid (Salpeter, 1969) and the mouse diaphragm (Salpeter, Plattner & Rogers, 1972) muscles, both the total DFP-reactive sites and the AChE sites were found to give rise in EM autoradiographs to grain distributions consistent with the location of those types of site either in the post-synaptic membrane or in the overlying cleft substance (although the pre-synaptic membrane as an *additional* source was not excluded in those studies). We have examined here the distribution of the DFP-reactive sites in relation to the folding of the membrane.

EM autoradiographs of ^3H -DFP-reacted mouse diaphragm, prepared in the previous study (Porter *et al.*, 1973*a*), were further analyzed by the method involved in Fig. 4. It was seen (Fig. 5) that the grains due to ^3H -DFP-reacted sites are found at an essentially uniform density from the crests to the base of the folds. The difference in distribution from the ^3H - α -BuTX-reacted sites is quite clear. There is a suggestion, in the ^3H -DFP case, that those sites are in fact *more* concentrated in the depths than in the primary cleft, but this possibility will need further analysis before weight can be given to it.

Salpeter *et al.* (1972) showed that the distribution of grains due to ^3H -DFP, when plotted with the axonal membrane as the (hypothetical) origin and including the grains in all regions, was skewed heavily towards the muscle side and was essentially the same for the total DFP-reactive sites as for the AChE sites. The fall-off of the labeling observed with positive distance from the hypothetical axonal origin (Salpeter *et al.*, 1972) was in each case distinctly less rapid than we find to be the case with ^3H - α -BuTX labeling in the same muscle type (Fig. 3*B*), again suggesting that neither the total ^3H -DFP-reactive nor the AChE sites are concentrated near the tips of the folds. The histograms obtained from our ^3H -DFP-reacted mouse diaphragm autoradiographs, if plotted for all grains from *either* the axonal *or* the postsynaptic membrane as origin (not illustrated here), are as shown for that muscle by Salpeter *et al.* (1972) for those two cases, respectively. Therefore, although we have not prepared 2-PAM-reactivated labeled specimens, we take the distribution of DFP-reacted sites along the folds,

shown in Fig. 5, to represent approximately, also, the relative distribution of the AChE sites along the folds. Hence, we conclude that AChE is present in the depths of the folds to a much greater degree than are the receptors. The data do not exclude the additional possibility that there is a greater concentration of the non-AChE DFP-reactive sites in the depths of the folds than there is of AChE.

Receptor Density in the Mouse Sternomastoid Endplate

A determination can also be made, by an indirect method, of the mean density of α -BuTX-binding sites at another endplate type, that of the mouse sternomastoid white fibers (Table 2). The average membrane density of the reaction sites of ^3H -diisopropylfluorophosphate (^3H -DFP) there is available from the determination of Salpeter *et al.* (1972). We also know the ratio (1.0) of ^3H -DFP-reactive sites to ^3H - α -BuTX binding sites at the same endplate type, from the autoradiographic analysis of Barnard *et al.* (1971) and Porter *et al.* (1973a). These ^3H -DFP-reactive sites can be used, therefore, as an internal standard to determine the membrane density of the receptor active centers. This determination is independent of the identity and exact location of the DFP-reactive sites, so long as the α -BuTX-binding sites are again postsynaptic, which seems a reasonable presumption for this second

Table 2. α -BuTX-binding sites at the postjunctional membrane and ultrastructural correlates, at three endplate types

Muscle Type	Fold depth (μ)	% Electron-dense region on PJM ^a	α -BuTX binding sites on PJM ^b	
			Mean density (per μ^2)	Density at crests (per μ^2)
Mouse diaphragm (red)	0.50	28	8,400	20-25,000
Mouse sternomastoid (white)	0.60	31 ^c	8,800	20-25,000
Bat diaphragm (red)	0.35	31	8,800	20-25,000

PJM, postjunctional membrane.

^a The area of the highly electron-dense or "thickened" region on the PJM (at and near the crests of the folds), expressed as a percentage of the total PJM, as measured on these electron-micrographs. "Crests" are as defined in Fig. 6.

^b The mean density value for the mouse diaphragm is from Porter *et al.* (1973a), by EM autoradiography and stereology. The mean density value for the mouse sternomastoid is calculated, and the maximum densities at the crests of the folds are derived, as stated in the present text.

^c Measured on 18 electron-micrographs of representative mouse sternomastoid endplate profiles.

mouse muscle. By this method, we obtained the same value for the average receptor site density as for the other two endplate types (Table 2).

Discussion

The results presented show that the cholinergic receptor sites at the bat red fiber endplate are located at the postjunctional membrane, at densities that are strikingly similar to that at the mouse red fiber endplate. In fact, for the three endplate types so far examined (Table 2), an average of 8,400 receptor sites/ μ^2 of postjunctional membrane was found.

The endplate α -BuTX-binding sites have been taken to be all of the ACh receptor sites in the present discussion, but previously (Porter *et al.*, 1973*b*) we pointed out that in studies here and elsewhere only 50–65% of these toxin-binding sites at the mammalian endplate had been shown to have the properties of the ACh receptor active center by other criteria, especially the binding of *d*-tubocurarine. This conclusion is amended, however, by recent studies of J. O. Dolly and E. A. Barnard (*in preparation*) which show that under appropriate conditions at least 90% of the endplate α -BuTX-binding sites *can* bind *d*-tubocurarine, with a dissociation constant of $10^{-6} - 10^{-7}$ M, and have other ligand properties of the receptor active center. Therefore, the values quoted here are close to the densities of true ACh receptor active centers. They do not, of course, specify entire receptor molecules, since the subunit composition of an endplate ACh receptor is as yet unknown.

Our results also show that the above-mentioned value represents an average density of sites for the entire postjunctional membrane, and that the true density at the crests of the folds is considerably higher. For the constancy of the average density to hold true for endplates with folds of different lengths, and having the observed form of receptor distribution, the area of increased density at the fold crests must cover a similar proportional area of the folds in each case. The depth of the fold, in that case, would not have a bearing on the average density of receptors for the entire membrane. The histograms for grain densities over the folds of the bat (Fig. 4) and the mouse (Fig. 5) endplates suggest that the extent of this zone is, in fact, proportional to the fold depth. The decline in grain density in descending the bat diaphragm endplate folds (average fold depth 0.35μ) is much more rapid than that in the mouse endplate, where they are deeper.

It appears, so far, that the zone of highest receptor density corresponds to the membrane regions of increased electron density ("thickenings") of the postjunctional folds, described previously by Birks *et al.* (1960) and

Table 3. Reported densities of intramembranous particles seen on the postsynaptic membrane of cholinergic synapses

Synapse	Particle structure (Å)	Particle arrangement	Particle density (per μ^2)	Authors
Rat endplates (various muscles)	110–140 (crests) 80–140 (depths)	irregular rows	1,800–2,300 at fold crests ~ 500 at fold depths	Rash & Ellisman (1974)
Frog sartorius endplates	80–120	plaques	~ 3,000 at fold crests ^b	Heuser <i>et al.</i> (1974)
<i>Torpedo</i> electroplaque	80–90 (5–6 subunits) ^a	regular arrays	12,000–15,000	Cartaud <i>et al.</i> (1973)
<i>Torpedo</i> electroplaque	80–90 (6 subunits) ^a	regular arrays	10,000	Potter & Nickel (1973)

^a Apparent number of subunits within each particle, as reported.

^b These occur in plaques of closely-packed particles which have a maximum density within them of 6,000 particles/ μ^2 . They occur all over the crest region, but are rare in the depths of the folds; the mean density of particles over the entire crest region (Fig. 6) may be roughly estimated at 3,000/ μ^2 (T. S. Reese, *personal communication*).

illustrated here in Fig. 1. We have measured this area in relation to the total postjunctional membrane, and find in representative electron-micrographs of the diaphragm and the sternomastoid endplates, that the highly electron-dense zone represents ~ 30% of the total traceable membrane profiles, even though the fold depths at these endplates vary considerably (Table 2). A constancy in binding site density, therefore, is thought to hold for the crest region in these three endplate types, as well as for the average density over all the postjunctional membrane in each. The significant grain density over portions of the folds distal from the axonal membrane (Fig. 4) suggests that the confinement of receptor molecules to the crests of the folds is not complete. Moreover, recent evidence from freeze-etch studies on characteristic postsynaptic intramembranous particles (*see* Table 3) indicates that the density of these is, at the depths of the folds, only about 1/6 that at the crests of the folds, in the case of the motor endplates. This value is compatible with the profile we find for receptor labeling (Figs. 4 and 5), suggesting that these particles carry the ACh receptors. From this value, and our observation that the electron-dense zone occupies 30% of the total postjunctional membrane, we calculate that the true receptor site density at the crests of folds is about 22,000 sites/ μ^2 . This estimate assumes a sharp demarcation between the receptor densities at the

tips and depths of the folds. It seems more likely that an intermediate gradient of receptor density, extending towards the fold depths, separates two extremes; however, the value of one-sixth of the maximum for the fold depths is an upper limit for that zone (*see* Results, and Table 3). The value of $22,000/\mu^2$ for the crests is approximate, and our results only indicate a range there of $20\text{--}25,000/\mu^2$. Similarly, Fertuck and Salpeter (1974), using $^{125}\text{I}\text{-}\alpha\text{-BuTX}$ -treated mouse sternomastoid muscle, recently noted (without quantitation) a heavily-labeled juxta-neuronal zone, but they report a demarcation from unlabeled fold depths.⁴

In the aforementioned studies with freeze-etch techniques, the particles characteristic of the vertebrate endplate postsynaptic membrane (Table 3) occur at the juxta-neuronal region of the folds of the endplate at an overall density there of $1,800\text{--}3,000/\mu^2$. We can compare this with our density of $20\text{--}25,000/\mu^2$ $\alpha\text{-BuTX}$ binding sites: if each of the particles carries a receptor complex that contains six $\alpha\text{-BuTX}$ -binding active centers, as is suggested by the observed number of subunits in various preparations (Table 3), this would predict a maximum of $18,000/\mu^2$ $\alpha\text{-BuTX}$ -binding sites at the crests. There may even be up to 12 $\alpha\text{-BuTX}$ sites per particle.

Estimates of the density of cholinergic receptor sites at synaptic membranes have also been made by other methods. The values reported vary considerably, and have been reviewed previously (Porter *et al.*, 1973*a*). We can note, however, that the mean values found for vertebrate motor endplates can all be reconciled with our present mean values when errors inherent in various methods are considered (Porter *et al.*, 1973*a*). One notable exception is the case of the electroplaque: the density of the intramembranous particles on the subsynaptic membrane of the *Torpedo* electroplaque is considerably greater (Table 3), but there is also a higher toxin-binding site density, i.e. $33,000/\mu^2$ as determined autoradiographically for the *Electrophorus* electroplaque (Bourgeois, Ryter, Menez, Fromageot, Boquet & Changeux, 1972). Hence, a true biological difference seems likely between the two types of cholinergic synapse (muscle endplate and electroplaque). The requirement for very rapid removal of receptor-bound ACh is less important in the electroplaque, but a high total conductance change is required, so a different distribution of the receptors there is understandable. If there are, indeed, six subunits per electroplaque postsynaptic particle and if each binds one $\alpha\text{-BuTX}$ molecule, then the density of $\alpha\text{-BuTX}$ -binding sites on the *Torpedo* postsynaptic membrane would have to be of the order of twice that of the already high density (Bourgeois *et al.*, 1972) on that of *Electrophorus*. Taking the known size of the electroplaque ACh receptor protein, this density would give a completely close-packed layer of receptor

protein alone (*see* Porter *et al.*, 1973*a* for the calculation). This raises the question whether the particle constitution in the electroplaque membrane is not different from that in the vertebrate endplate.

The finding that the ACh receptor sites are concentrated mainly at the crests of the folds in the endplate raises a more general question about these structures—namely, what function they serve in synaptic physiology. Clearly, since only a portion of the folds is covered by receptors, their purpose is not, as has previously often been thought, to provide an increased membrane surface area to accommodate the receptor. Further, the folds do not serve simply to concentrate the receptors at the endplate region, since the density found in this study for the sarcolemma (Table 1) is only a fraction of that at the synaptic membrane, even though the two are continuous. An analysis of ^3H -DFP binding at the endplate (Fig. 5) provides some insight into the fold function. As already noted (p. 40), this binding reveals also the distribution, essentially, of the AChE molecules. This enzyme is thought to reside in the cleft substance, since removal of the latter with proteolytic enzymes (Betz & Sakmann, 1971; Hall & Kelly, 1971) also banishes AChE activity. Fig. 5 shows that at mouse diaphragm endplates labeled with ^3H -DFP, the grain density distribution is essentially uniform over the folds. Moreover, the cleft substance layer involved can be seen, in well-preserved EM thin sections, to extend right to the bottom of each fold. We have, then, a situation wherein the lower two-thirds or so of each fold is rich in AChE but is relatively sparse in receptors. The postsynaptic cleft region above this (*i.e.* towards the presynaptic side) is rich in both components. On this design, those ACh molecules which do not diffuse out of the cleft fast enough because they are near the base of a fold can find a zone where receptor encounters are rare but enzymic encounters are very frequent. This situation would be needed, given a well-folded membrane, for high-frequency firing. The reason for the secondary folding *per se* might be suggested to lie in providing a more rapid conductance channel for the wave of postsynaptic membrane depolarization to the sarcolemma and myofibrils; this could be a feature needed in thicker “white” fibers which are commonly the site (Zacks, 1973) of the most extensive synaptic folding. Whether those postsynaptic membrane regions that are sparse in receptors are also electrogenic in constitution is as yet uncertain. Certainly, the walls of the folds in fast fiber frequently anastomose (Ogata & Murata, 1972; Fardeau, 1973) and appear to establish a lateral continuity with the sarcolemma. One should also consider the report of Zacks and Saito (1970) that connections exist at the depths of the secondary folds to the sarcoplasmic tubular system: if characteristic, these would provide an alternative ex-

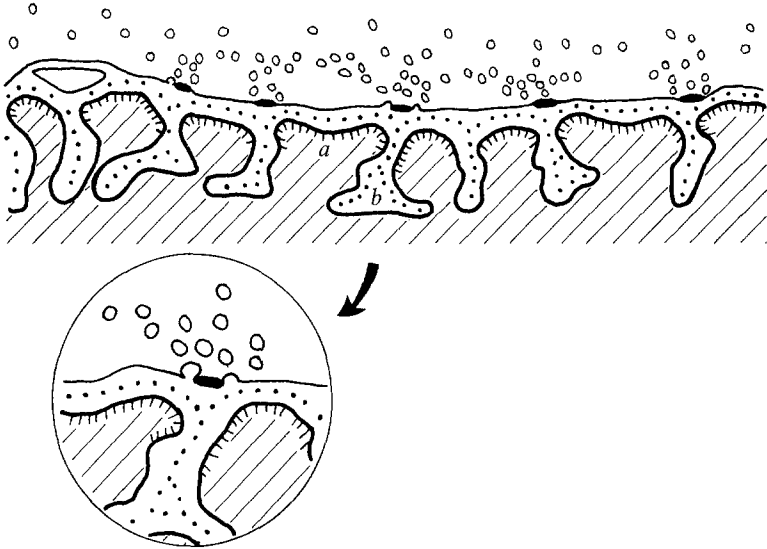


Fig. 6. Interpretative diagram of part of the subneural apparatus of the frog motor endplate, to show the spatial relationships between sites of transmitter release and receptor concentrations. In the terminal axon, the presynaptic vesicles become aligned in stacks apposing the mouths of the postsynaptic folds (Birks *et al.*, 1960). Traced from micrographs of frog muscle endplates (Couteaux & Pecot-Dechavassine, 1968). The striations along the postsynaptic membrane represent its "thickened" zone, rich in the receptors (i.e., the region referred to in the text as a "crest"). In the mammalian white fibers, the folds are usually more closely spaced than here, so that the crests are narrower and apical. Dense bars on the presynaptic membrane represent the ridges seen in freeze-etch preparations. Dotted lines show the extent of the stainable cleft substance, and, it is presumed, of the AChE.

The inset, showing at higher magnification the release of a vesicle, is based on the presynaptic geometry of stimulated endplates, as determined by Couteaux and Pecot-Dechavassine (1970) and Heuser *et al.* (1974). A presynaptic ridge, seen here in cross-section as a dense amorphous zone, is associated with paired sites of vesicle release. This ridge prevents the vesicles from releasing transmitter directly into the receptor-poor region of the fold depths (*b*). Instead, the vesicles fuse with the presynaptic membrane in a specific region on either side of the ridge (the "zones actives" of Couteaux), so that the transmitter is expelled onto the receptor-rich crests of the folds (*a*). We propose that upon release from the receptors, that fraction of the ACh which does not immediately diffuse to the exterior, and which would otherwise tend to linger towards the base of each fold, is in a region which is poor in receptors but rich in acetylcholinesterase, so that it is hydrolyzed before it can give rise to excessive activation of receptors.

planation for the facilitation of conduction of excitation by synaptic folds on a thick muscle fiber. Another conceivable reason for these receptor-poor regions could be that they are the sites of ion-pumping systems in the membrane, needed for recovery of ions exchanged into the synaptic cleft.⁵

Another significant consideration concerns the most effective deployment of receptor molecules with respect to the transmitter packets released from the nerve terminal. In fact, at first sight the arrangement discovered here would seem to be unsuitable for a high efficiency of combination of ACh with receptors. The presynaptic ACh-containing vesicles concentrate themselves in small stacks over the mouths of the subsynaptic folds (Birks *et al.*, 1960; Couteaux & Pecot-Dechavassine, 1970). Characteristic "vesicle release sites" (*see* Fig. 6) on the presynaptic membrane can be discerned there (Couteaux & Pecot-Dechavassine, 1970; Pfenninger, Akert, Moor & Sandri, 1972; Dreyer, Peper, Akert, Sandri & Moor, 1973; Fardeau, 1973; Heuser & Reese, 1973; Heuser, Reese & Landis, 1974). Vesicles are observed to attach at these sites in the process of release. This would seem to indicate that ACh is expelled down into each fold. Why, then, are there so few receptors down in the folds? Recent detailed examinations by freeze-fracture techniques provide an answer to this question. An electron-dense ridge occurs at each vesicle site on the presynaptic membrane; vesicles cluster in the neuroplasm around these ridges, and in stimulated terminals the process of vesicle attachment and discharge can be seen at specific sites at each side of a ridge (Heuser *et al.*, 1974). As shown in Fig. 6B, this arrangement ensures that, in fact, the vesicle contents are expelled onto the crest of each folded postsynaptic unit, and do not have a direct path into the mouth of the fold. Hence, the zone of concentration of receptor sites found here matches well the presynaptic assembly for transmitter release.

The constancy of both the crest density of ACh receptors and the form of their distribution over the folds, in the muscles of the two species studied here, encourages the view that this arrangement is a universal feature of the endplate. While the bat is in a different order of mammals to the rodents, wider comparisons will have to be made to establish its universality in the vertebrates. The question must be raised whether a universality, even in the mammalian muscles alone, of ACh receptor content in the endplate postsynaptic membrane would hold for their *mean* membrane density: the endplate types so far examined have all been fairly rich in folds, and the mean value may not be the generally significant one. It must be investigated whether, instead, the high density in the postsynaptic regions closest to the axon is the characteristic parameter for receptor function.

This work was supported by Grant GM-11754 of the U.S. National Institutes of Health. During this study, C.W.P. was supported by Experimental Pathology Training Grant No. 01500 from the National Institute of General Medical Sciences. Dr. T. H. Chiu of this laboratory prepared and characterized the sample of ^3H - α -bungarotoxin used. We are grateful to Dr. F. C. Kallen for providing the bat, and Dr. G. C. Budd (Toledo, Ohio) for kindly determining the sensitivity of our emulsion.

Notes Added in Proof:

⁴ While this paper was in press, further evidence from freeze-etch studies of endplate membranes was published by K. Peper, F. Dreyer, C. Sandri, K. Akert and H. Moor (*Cell Tiss. Res.* **149**:437, 1974). In the frog cutaneous pectoris muscle, the postsynaptic membrane contained intramembranous particles in local aggregations of 7,500/ μ^2 density. These dense patches, of variable extent, were seen only in that area of the folds nearest to the presynaptic "active zones", i.e. in the crest region in our terminology. Similar particles are reported on the lower 75% of the walls of the folds, but not in such patches, and occurring with "relative paucity". Further, the precise alignment of the postsynaptic fold crests with the vesicle attachment sites which occur at the edges of the "active zones" of the presynaptic membrane can be clearly seen in their micrographs.

⁵ In a recent paper, S. Thesleff, F. Vyskocil and M. P. Ward (*Acta Physiol. Scand.* **91**:196, 1974) show that the endplate in the rat diaphragm (and similar results have also been reported for the frog sartorius endplate) contains local postsynaptic sites of regenerative electrical response, which differ (e.g. in being tetrodotoxin-resistant) from the classical regenerative sites of the sarcolemma. The possibility that regenerative action occurs in the fold depths must, therefore, continue to be considered.

References

- Albuquerque, E. X., Barnard, E. A., Chiu, T. H., Lapa, A. J., Dolly, J. O., Jansson, S. E., Daly, J., Witkop, B. 1973. Ionic conductance modulator and acetylcholine receptor sites in the mouse neuromuscular junction: Evidence from specific toxin reactions. *Proc. Nat. Acad. Sci.* **70**:949
- Albuquerque, E. X., Barnard, E. A., Porter, C. W., Warnick, J. E. 1974. The density of acetylcholine receptors and their sensitivity in the postsynaptic membrane of muscle endplates. *Proc. Nat. Acad. Sci.* **71**:2818
- Barnard, E. A., Rogers, A. W. 1967. Determination of the number, distribution and some *in situ* properties of cholinesterase molecules at the motor end-plate, using labeled inhibitor methods. *Ann. N.Y. Acad. Sci.* **144**:584
- Barnard, E. A., Wieckowski, J., Chiu, T. H. 1971. Cholinergic receptor molecules and cholinesterase molecules at mouse skeletal muscle junctions. *Nature* **234**:207
- Betz, W., Sakmann, B. 1971. "Disjunction" of frog neuromuscular synapses by treatment with proteolytic enzymes. *Nature, New Biol.* **232**:94
- Birks, R. I., Huxley, H. E., Katz, B. 1960. The fine structure of the neuromuscular junction of the frog. *J. Physiol. (London)* **150**:134
- Bourgeois, J.-P., Rytter, A., Menez, A., Fromageot, P., Boquet, P., Changeux, J.-P. 1972. Localization of the cholinergic receptor protein in *Electrophorus* electroplax by high resolution autoradiography. *FEBS Lett.* **25**:127
- Cartaud, J., Beneditt, E. L., Cohen, J. B., Meunier, J.-C., Changeux, J.-P. 1973. Presence of a lattice structure in membrane fragments rich in nicotinic receptor protein from electric organ of *Torpedo marmorata*. *FEBS Lett.* **33**:109
- Chiu, T. H., Lapa, A. J., Barnard, E. A., Albuquerque, E. X. 1974. Binding of d-tubocurarine and α -bungarotoxin in normal and denervated mouse muscles. *Exp. Neurol.* **43**:399
- Couteaux, R., Pecot-Dechavassine, M. 1968. Particularites structurales du sarcoplasme sous-neural. *Compt. Rend. Acad. Sci. (Ser. D), Paris* **266**:8
- Couteaux, R., Pecot-Dechavassine, M. 1970. Vesicules synaptiques et poches au niveau des "zones actives" de la jonction neuromusculaire. *Comp. Rend. Acad. Sci. (Ser. D), Paris* **271**:2346

- Dreyer, F., Peper, K., Akert, K., Sandri, C., Moor, H. 1973. Ultrastructure of the "active zone" in the frog neuromuscular junction. *Brain Res.* **62**:373
- Fardeau, M. 1973. Normal ultrastructural aspects of human motor endplate and its pathologic modifications. *In: The Striated Muscle.* C. M. Pearson and F. K. Mostofi, editors. p. 342. Williams & Wilkins Co., Baltimore
- Fertuck, H. C., Salpeter, M. M. 1974. Localization of acetylcholine receptor by ¹²⁵I-labeled α -bungarotoxin binding at mouse motor endplates. *Proc. Nat. Acad. Sci.* **71**:1376
- Gauthier, G. F., Padykula, H. A. 1966. Cytological studies of fiber types in skeletal muscle. A comparative study of the mammalian diaphragm. *J. Cell Biol.* **28**:333
- Hall, Z. W., Kelly, R. B. 1971. Enzymatic detachment of endplate acetylcholinesterase from muscle. *Nature, New Biol.* **232**:62
- Heuser, J. E., Reese, T. S. 1973. Evidence for recycling of synaptic vesicle membrane during transmitter release at the frog neuromuscular junction. *J. Cell Biol.* **57**:315
- Heuser, J. E., Reese, T. S., Landis, D. M. D. 1974. Functional changes in frog neuromuscular junctions studied with freeze-fracture. *J. Neurocytol.* **3**:109
- Lee, C. Y. 1972. Chemistry and pharmacology of polypeptide toxins in snake venoms. *Annu. Rev. Pharmacol.* **12**:265
- Ogata, T., Murata, F. 1969. Fine structure of motor endplate in red, white and intermediate fibers of mammalian fast muscle. *Tohoku J. Exp. Med.* **98**:107
- Pfenninger, K., Akert, K., Moor, H., Sandri, C. 1972. The fine structure of freeze-fractured presynaptic membranes. *J. Neurocytol.* **1**:129
- Porter, C. W., Barnard, E. A. 1974. Electron microscope autoradiographic counting of acetylcholine receptor sites in mammalian motor endplates. *J. Histochem. Cytochem.* **22**:293
- Porter, C. W., Barnard, E. A., Chiu, T. H. 1973a. The ultrastructural localization and quantitation of cholinergic receptors at the mouse motor endplate. *J. Membrane Biol.* **14**:383
- Porter, C. W., Chiu, T. H., Wieckowski, J., Barnard, E. A. 1973b. Types and locations of cholinergic receptor-like molecules in muscle fibres. *Nature, New Biol.* **241**:3
- Potter, L. T., Nickel, E. 1973. Fine structure of postsynaptic membranes in *Torpedo* electric tissue. *J. Cell Biol.* **59**:246a
- Rash, J. E., Ellisman, M. H. 1974. Studies of excitable membranes. I. Macromolecular specializations of the neuromuscular junction and the nonjunctional sarcolemma. *J. Cell Biol.* **63**:567
- Salpeter, M. M. 1969. Electron microscope radioautography as a quantitative tool in enzyme cytochemistry. II. The distribution of DFP-reactive sites at motor endplates of a vertebrate twitch muscle. *J. Cell Biol.* **42**:122
- Salpeter, M. M., Bachmann, L., Salpeter, E. E. 1969. Resolution in electron microscope radioautography. *J. Cell Biol.* **41**:1
- Salpeter, M. M., Plattner, H., Rogers, A. W. 1972. Quantitative assay of esterases in endplates of mouse diaphragm by electron microscope autoradiography. *J. Histochem. Cytochem.* **20**:1059
- Zacks, S. I. 1973. *The Motor Endplate.* R. E. Krieger Publishing Co., Huntington, N.Y.
- Zacks, S. I., Saito, A. 1970. Direct connections between the T system and the subneural apparatus in mouse neuromuscular junctions demonstrated by lanthanum. *J. Histochem. Cytochem.* **18**:302